

ATTITUDE TRACKING CONTROL FOR SPACECRAFT FORMATION FLYING

Matthew R. Long and Christopher D. Hall
Aerospace and Ocean Engineering
Virginia Polytechnic Institute and State University

ABSTRACT

We develop a non-linear tracking control law to be applied to formation flying spacecraft. Each spacecraft in the formation is modeled as a rigid body with N axisymmetric wheels controlled by axial torques, and the kinematics are represented by Modified Rodrigues Parameters (MRPs). The paper first derives the open-loop reference attitude, rate, and acceleration commands for tracking a moving object with the sensor boresight vector defined along a body-fixed axis. The reference trajectory is constructed so that the solar panel normal is aligned with the sun vector at all times while tracking targets on the rotating earth. The controller makes the body frame asymptotically track the reference motion when there are initial errors in the position and angular rates. A simple target tracking example is presented to demonstrate that the controller will allow each spacecraft in the formation to track the target and the sun simultaneously.

INTRODUCTION

The formation flying concept has become a topic of interest in recent years. Gramling et al.¹ discussed the On-board Navigation System (ONS) for relative navigation of the Earth-Observing-1 (EOS-1)/Landsat-7 (L-7) formation. The performance of the ONS was investigated in terms of tracking measurement type and quality, tracking frequency, and the relative orbital geometry of the formation. DeCou² presented a station-keeping strategy for formation flying interferometry. He discussed the basic orbital configuration for interferometry missions and the thrust requirements for station-keeping of a two-satellite formation. The work done by Ulybyshev³ pertains to station-keeping of a constellation using a linear-quadratic regulator for feedback control. The controller minimized the along-track relative displacements between spacecraft and the orbital period displacements relative to a reference orbit. Folta et al.⁴ also addressed separations between spacecraft in a formation. The performance of a formation to observe ground targets simultaneously for various separations was evaluated. Simulation results for three different types of formations were presented in terms of attitude and field of view (FOV) errors.

Spacecraft rotational tracking maneuvers specifically for formation flying have not been addressed in the literature. The problem of tracking moving objects applicable to formation flying has been studied by various authors, and much of the work developed in this paper is based on Refs. 5, 6 and 7. Schaub et al.⁸ also discussed rotational tracking maneuvers similar to what we present here, except that they optimized the reference trajectory for time and fuel requirements and used a different Lyapunov function to derive the momentum wheel controller. Steyn⁹ and Wie and Lu¹⁰ both investigated momentum wheel feedback controllers for rotational maneuvers. Slew rate constraints and near-minimum-time maneuvers were taken into account.

To determine the feasibility of formation simultaneous target tracking, we first consider the pointing and tracking requirements for an individual spacecraft. The desired attitude is constructed by making the sensor boresight axis co-linear with the position vector from the spacecraft to any arbitrary target. We define the target to be a point on the rotating earth, but it could be any inertially fixed, or moving target. We define two intermediate coordinate frames using the boresight axis, the solar array axis, and the sun vector to construct basis vectors that simultaneously allow the spacecraft to point at the target and keep the solar panel vector normal to the sun direction. The ideal tracking body rates and accelerations are computed from the first and second derivatives of the attitude, respectively. The reference acceleration is used to compute the ideal axial control torque for the control law. The controller uses Lyapunov control theory to drive any initial errors in the attitude and angular velocity to zero asymptotically. The

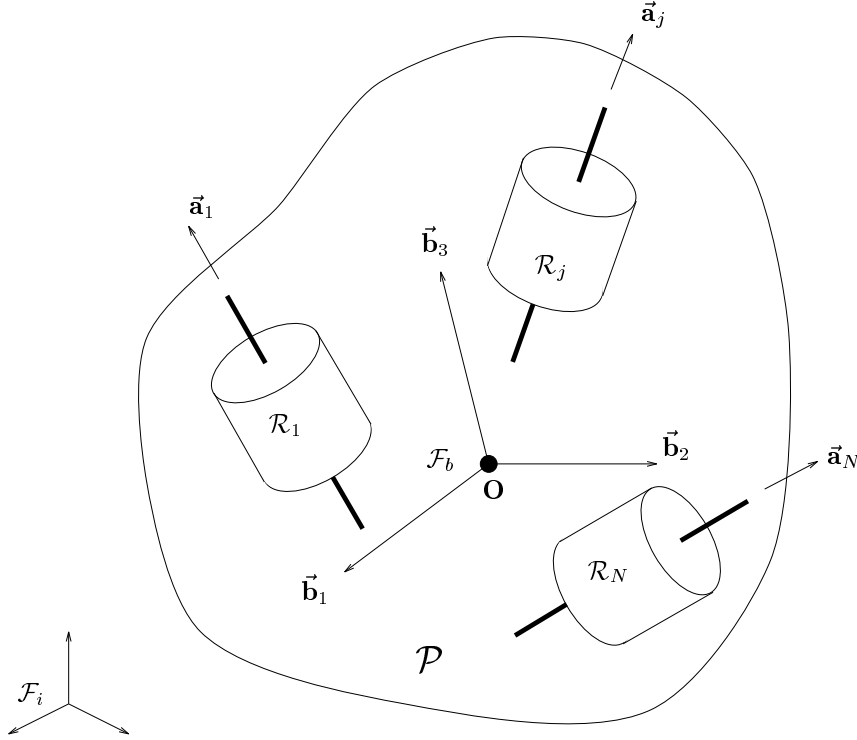


Figure 1: Rigid body with N momentum wheels

controller calculates the necessary control torque to track the specified trajectory, while countering all effects due to gravity gradient torques.

The first part of this paper defines the equations of motion an individual formation flying spacecraft model. The dynamics are presented, along with the kinematics expressed in terms of the body and reference frames. The second part of the paper outlines the open-loop computation of the ideal target tracking trajectory while keeping perfect alignment between the solar panel normal and the sun. The last part of the paper deals with the nonlinear feedback controller that makes the spacecraft body frame track the reference trajectory.

EQUATIONS OF MOTION

In this section, a system model is presented for use in developing tracking control algorithms. The equations of motion presented here follow the notation developed in Hughes¹¹ and Hall.¹² We first consider a rigid spacecraft P , shown in Figure 1, with N rigid momentum wheels W_i , $i = 1, \dots, N$. The wheels have an arbitrary, but fixed orientation with respect to the body. Let \mathcal{F}_b denote the body frame with the origin at the center of mass of the system $P + \sum_{i=1}^N W_i$, and \mathcal{F}_i denote the inertial frame. The desired trajectory to be tracked comes from the trajectory generated by a “virtual” spacecraft in a reference frame. Let \mathcal{F}_r represent this reference frame which is fixed at the center of mass of this virtual spacecraft. In Ref. 7, the “virtual” spacecraft is assumed to be a rigid body. Here we assume that the virtual spacecraft is a rigid body with momentum wheels, *i.e.* a gyrostat, with the same properties as the real spacecraft.

Let \mathbf{I} represent the moment of inertia of the system, including the momentum wheels, and $\mathbf{I}_s = \text{diag}\{I_{s1}, \dots, I_{sN}\}$ denote the axial moments of inertia of each momentum wheel. The dynamics of the gyrostat are given by

$$\dot{\mathbf{h}}_b = \mathbf{h}_b^\times \mathbf{J}^{-1} (\mathbf{h}_b - \mathbf{A} \mathbf{h}_a) + \mathbf{g}_e \quad (1)$$

$$\dot{\mathbf{h}}_a = \mathbf{g}_a \quad (2)$$

$$\dot{\boldsymbol{\sigma}}_b = \mathbf{G}(\boldsymbol{\sigma}_b)\boldsymbol{\omega}_b \quad (3)$$

where “ \times ” denotes a skew-symmetric matrix, \mathbf{h}_b is the 3×1 system angular momentum vector in \mathcal{F}_b

$$\mathbf{h}_b = \mathbf{I}\boldsymbol{\omega}_b + \mathbf{A}\mathbf{I}_s\boldsymbol{\omega}_s \quad (4)$$

and \mathbf{h}_a is the $N \times 1$ matrix of the axial angular momenta of the wheels defined as

$$\mathbf{h}_a = \mathbf{I}_s\mathbf{A}^T\boldsymbol{\omega}_b + \mathbf{I}_s\boldsymbol{\omega}_s \quad (5)$$

Here $\boldsymbol{\omega}_s$ is an $N \times 1$ matrix that describes the axial angular velocities of the momentum wheels relative to the body. The $3 \times N$ matrix \mathbf{A} contains the axial unit vectors of the N momentum wheels, and \mathbf{J} is an inertia-like matrix¹² defined as

$$\mathbf{J} = \mathbf{I} - \mathbf{A}\mathbf{I}_s\mathbf{A}^T \quad (6)$$

From Eqs. (4), (5), and (6) it can be shown that the angular velocity of the body frame can be written as

$$\boldsymbol{\omega}_b = \mathbf{J}^{-1}(\mathbf{h}_b - \mathbf{A}\mathbf{h}_a) \quad (7)$$

The term \mathbf{g}_a represents the $N \times 1$ matrix of the internal axial torques applied by the platform to the momentum wheels. This is the control torque needed for tracking maneuvers. In this paper, the only external torque that our controller compensates for is the uncontrolled gravity gradient torque¹³ \mathbf{g}_e :

$$\mathbf{g}_e = 3 \frac{\mu}{\|\mathbf{r}_{so}\|^3} \hat{\mathbf{o}}_3^\times \mathbf{I} \hat{\mathbf{o}}_3 \quad (8)$$

where $\hat{\mathbf{o}}_3$ is the nadir vector, *i.e.* $\hat{\mathbf{o}}_3 = -\mathbf{r}_{so}/\|\mathbf{r}_{so}\|$, with \mathbf{r}_{so} being the position vector from the center of the earth to the center of mass of the spacecraft in the orbital frame \mathcal{F}_o . The kinematics in Eq. (3) are written in terms of Modified Rodrigues Parameters (MRP's). The MRP's are a three-parameter set derived from the Euler axis/angle representation¹⁴ and are defined:

$$\boldsymbol{\sigma} = \hat{\mathbf{e}} \tan(\Phi/4) \quad (9)$$

where $\hat{\mathbf{e}}$ is the unit vector along the Euler principal axis, and Φ is the Euler principal rotation angle. The matrix $\mathbf{G}(\boldsymbol{\sigma}_b)$ in Eq. (3) is defined as

$$\mathbf{G}(\boldsymbol{\sigma}_b) = \frac{1}{2} \left(\mathbf{1} + \boldsymbol{\sigma}_b^\times + \boldsymbol{\sigma}_b^T \boldsymbol{\sigma}_b - \frac{1 + \boldsymbol{\sigma}_b^T \boldsymbol{\sigma}_b}{2} \mathbf{1} \right) \quad (10)$$

where $\mathbf{1}$ is the 3×3 identity matrix.

Since the virtual spacecraft has the same inertial and wheel parameters as the real spacecraft, the reference frame dynamics are the same as Eqs. (1–5), except that the subscript b is replaced with r . The uncontrolled external torque \mathbf{g}_e remains the same and the reference wheel torque \mathbf{g}_{ar} comes from first noting that $\dot{\mathbf{h}}_r$ can also be expressed as

$$\dot{\mathbf{h}}_r = \mathbf{J}\dot{\boldsymbol{\omega}}_r + \mathbf{A}\dot{\mathbf{h}}_{ar} = \mathbf{J}\dot{\boldsymbol{\omega}}_r + \mathbf{A}\mathbf{g}_{ar} \quad (11)$$

Equating Eqs. (11) and (1) in terms of \mathcal{F}_r yields the following expression for the desired axial control torque $\mathbf{A}\mathbf{g}_{ar}$:

$$\mathbf{A}\mathbf{g}_{ar} = \mathbf{h}_r^\times \mathbf{J}^{-1}(\mathbf{h}_r - \mathbf{A}\mathbf{h}_{ar}) + \mathbf{g}_e - \mathbf{J}\dot{\boldsymbol{\omega}}_r \quad (12)$$

where $\mathbf{J}^{-1}(\mathbf{h}_r - \mathbf{A}\mathbf{h}_{ar})$ is the desired angular velocity $\boldsymbol{\omega}_r$. The torque \mathbf{g}_{ar} is the torque that would generate the desired trajectory without any initial condition errors. Likewise with the kinematics, the reference MRP's are given by Eq. (3) with the subscript r instead of b .

TRACKING KINEMATICS

Tracking a moving object involves two kinematical aspects: pointing at an object and then moving at the correct rate to stay aligned with the target for a given length of time. In this section, we develop the ideal attitude, rate, and acceleration commands needed for target tracking. The desired trajectory is computed in an open-loop fashion, and is defined to be the trajectory of the virtual spacecraft in \mathcal{F}_r . The controller will then make the body frame track this reference motion asymptotically.

Pointing

Pointing at a target requires a specific attitude to make the position vector from the target to the spacecraft co-linear with the instrument boresight as illustrated in Fig. 2. We define the target to be a point on the rotating earth defined by its latitude and longitude. We also require that the attitude be constructed so that the sun unit vector \hat{s} is perpendicular to the solar panel unit vector \hat{p} while pointing at the target. This sun tracking is also known as yaw-steering.¹⁵

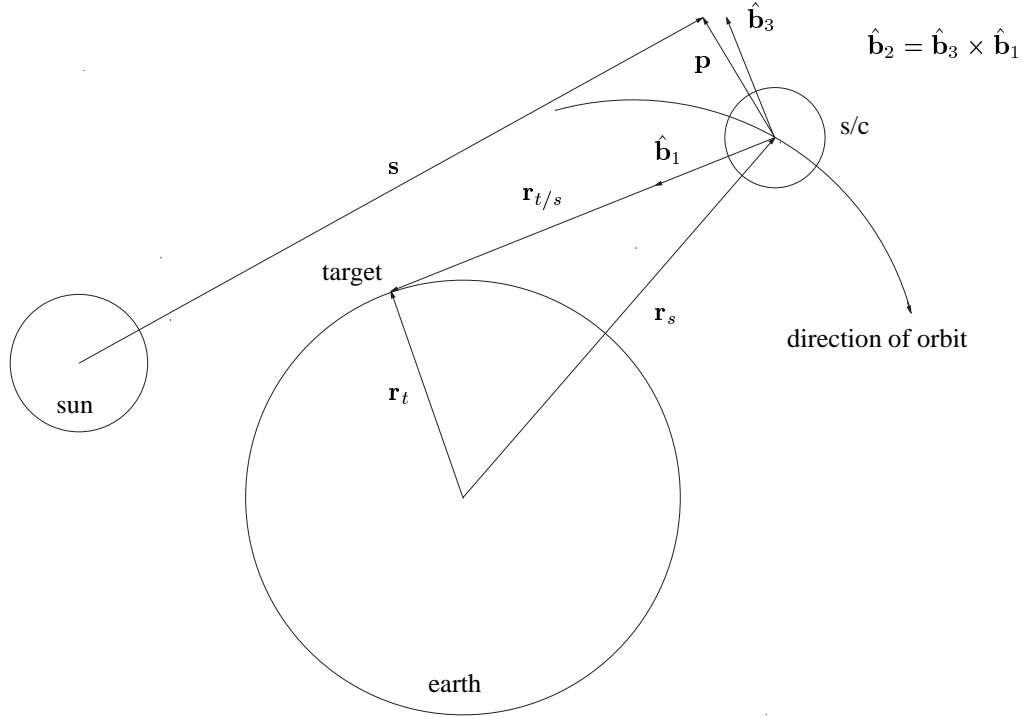


Figure 2: Setup for Target Tracking.

The instrument axis can be any unit vector fixed in \mathcal{F}_b , which is defined to be the same in \mathcal{F}_r . In this paper, we assume that the instrument boresight is defined along the “1” direction in \mathcal{F}_b and \mathcal{F}_r :

$$\mathbf{a}_b = \mathbf{a}_r = [1 \ 0 \ 0]^T \quad (13)$$

From Figure 2, it can easily be seen that the target position vector with respect to the spacecraft, $\mathbf{r}_{t/s}$, can be written in \mathcal{F}_i as

$$\mathbf{r}_{t/si} = \mathbf{r}_{ti} - \mathbf{r}_{si} \quad (14)$$

where \mathbf{r}_{ti} represents the position vector from the center of the earth to the spacecraft in \mathcal{F}_i . The vector \mathbf{r}_{si} is assumed known, and the target position vector is expressed in \mathcal{F}_i as

$$\mathbf{r}_{ti} = [\cos(\delta_t) \cos(\theta_{GST} + L_t) \quad \cos(\delta_t) \sin(\theta_{GST} + L_t) \quad \sin(\delta_t)]^T \quad (15)$$

where δ_t and L_t are the latitude and longitude of target, respectively, and θ_{GST} is Greenwich sidereal time measured from a given epoch.

To find the required pointing attitude, we develop the rotation matrix \mathbf{R}^{ri} that will make the condition in Fig. (2) true and satisfy the yaw-steering condition:

$$\hat{s} \cdot \hat{\mathbf{p}}_r = 0 \quad (16)$$

We define two intermediate frames \mathcal{F}_a and \mathcal{F}_c that are used with the frames \mathcal{F}_o and \mathcal{F}_r to construct the rotation matrix \mathbf{R}^{ri} . Our motivation for this approach is that given the position vectors in Figure 2, \mathbf{a} , $\hat{\mathbf{s}}$, and $\hat{\mathbf{p}}$, the attitude that will align the boresight with the target and the solar panel normal with the sun can be constructed at once by the following:

$$\mathbf{R}^{ri} = \mathbf{R}^{rc} \mathbf{R}^{ca} \mathbf{R}^{ao} \mathbf{R}^{oi} \quad (17)$$

An alternative method is to develop the necessary pointing attitude without the yaw steering, and then determine the rotation about the sensor axis needed to satisfy Eq. (16). This approach is less attractive since it requires an extra computation in the algorithm.

The rotation matrix \mathbf{R}^{oi} is determined by the spacecraft inertial position and velocity vectors \mathbf{r}_{si} and \mathbf{v}_{si} , respectively, and is given by the following

$$\hat{\mathbf{o}}_{3i} = \frac{-\mathbf{r}_{si}}{\|\mathbf{r}_{si}\|} \quad (18)$$

$$\hat{\mathbf{o}}_{2i} = \frac{\mathbf{r}_{si}^\times \mathbf{v}_{si}}{\|\mathbf{r}_{si}^\times \mathbf{v}_{si}\|} \quad (19)$$

$$\hat{\mathbf{o}}_{1i} = \frac{\hat{\mathbf{o}}_{2i}^\times \hat{\mathbf{o}}_{3i}}{\|\hat{\mathbf{o}}_{2i}^\times \hat{\mathbf{o}}_{3i}\|} \quad (20)$$

$$\mathbf{R}^{oi} = [\hat{\mathbf{o}}_{1i} \ \hat{\mathbf{o}}_{2i} \ \hat{\mathbf{o}}_{3i}]^T \quad (21)$$

We construct the basis of \mathcal{F}_a using the boresight axis \mathbf{a} and the sun vector $\hat{\mathbf{s}}$. These vectors, known in the orbital frame using Eq. (21), are used to construct the rotation matrix \mathbf{R}^{ao} . As with \mathbf{R}^{oi} , the rotation matrix between \mathcal{F}_o and \mathcal{F}_a is

$$\hat{\mathbf{a}}_{1o} = \mathbf{a}_o \quad (22)$$

$$\hat{\mathbf{a}}_{3o} = \frac{\mathbf{a}_o^\times \hat{\mathbf{s}}_o}{\|\mathbf{a}_o^\times \hat{\mathbf{s}}_o\|} \quad (23)$$

$$\hat{\mathbf{a}}_{2o} = \hat{\mathbf{a}}_{3o}^\times \hat{\mathbf{a}}_{1o} \quad (24)$$

$$\mathbf{R}^{ao} = [\hat{\mathbf{a}}_{1o} \ \hat{\mathbf{a}}_{2o} \ \hat{\mathbf{a}}_{3o}]^T \quad (25)$$

The basis of \mathcal{F}_c is defined by the solar panel axis $\hat{\mathbf{p}}$, and the boresight axis vector \mathbf{a} , both of which are known in \mathcal{F}_b and hence, \mathcal{F}_r . As before, the rotation matrix \mathbf{R}^{rc} is constructed by

$$\hat{\mathbf{c}}_{1r} = \mathbf{a}_r \quad (26)$$

$$\hat{\mathbf{c}}_{3r} = \frac{\mathbf{a}_r^\times \hat{\mathbf{p}}_r}{\|\mathbf{a}_r^\times \hat{\mathbf{p}}_r\|} \quad (27)$$

$$\hat{\mathbf{c}}_{2r} = \hat{\mathbf{c}}_{3r}^\times \hat{\mathbf{c}}_{1r} \quad (28)$$

$$\mathbf{R}^{rc} = [\hat{\mathbf{c}}_{1r} \ \hat{\mathbf{c}}_{2r} \ \hat{\mathbf{c}}_{3r}]^T \quad (29)$$

To determine the rotation matrix from \mathcal{F}_c to \mathcal{F}_a , we use the prescribed orthogonality condition between the sun vector and the solar panel axis. Equation (16) can be expressed as

$$\hat{\mathbf{s}}_a^T \mathbf{R}^{ac} \hat{\mathbf{p}}_c = 0 \quad (30)$$

From Eqs. (22) and (26), it is easy to see that $\hat{\mathbf{a}}_1$ and $\hat{\mathbf{c}}_1$ are the same vector, therefore $\hat{\mathbf{a}}_1 \cdot \hat{\mathbf{c}}_1 = 1$. By definition, the unit vectors $\hat{\mathbf{a}}_2$ and $\hat{\mathbf{a}}_3$ are perpendicular to $\hat{\mathbf{a}}_1$, so they are also perpendicular to $\hat{\mathbf{c}}_1$. The same is true for $\hat{\mathbf{a}}_1$, which is also perpendicular to $\hat{\mathbf{c}}_2$ and $\hat{\mathbf{c}}_3$. As a result, \mathbf{R}^{ac} is a "1" rotation and Eq. (30) becomes

$$\hat{\mathbf{s}}_a^T \begin{bmatrix} 1 & 0 & 0 \\ 0 & \cos \theta_{ac} & \sin \theta_{ac} \\ 0 & -\sin \theta_{ac} & \cos \theta_{ac} \end{bmatrix} \hat{\mathbf{p}}_c = 0 \quad (31)$$

Because of the way we have defined \mathcal{F}_a and \mathcal{F}_c , s_{3a} and p_{3c} are zero and Eq. (31) expands as

$$s_{1a}p_{1c} + s_{2a}p_{2c} \cos \theta_{ac} = 0 \quad (32)$$

The angle θ_{ac} is then easily found by solving Eq. (32), which satisfies the yaw-steering condition. \mathbf{R}^{ac} is then calculated by substituting θ_{ac} into Eq. (31). The ideal target pointing attitude \mathbf{R}^{ri} is then constructed by multiplying together the rotation matrices found in Eq. (17).

Tracking

To keep the spacecraft pointed at the target, the spacecraft must rotate as it moves in its orbit. We develop rate and acceleration commands similar to those found in Ref. 6. We begin by taking a time derivative of Eq. (14) to get

$$\dot{\mathbf{r}}_{t/si} = \dot{\mathbf{r}}_{ti} - \dot{\mathbf{r}}_{si} \quad (33)$$

where $\dot{\mathbf{r}}_{si}$ is simply the known spacecraft velocity vector and $\dot{\mathbf{r}}_{ti}$ is given by $\boldsymbol{\omega}_e^\times \mathbf{r}_{ti}$, where $\boldsymbol{\omega}_e$ is the angular velocity of the earth.

For the spacecraft to track a given target correctly, the angular velocity has to be coupled to the attitude. We preserve this coupling by calculating the spacecraft angular rate vectors in each of the coordinate frames and then use the pieces to construct the correct angular tracking rate in the body frame, which is

$$\boldsymbol{\omega}_r^{ri} = \boldsymbol{\omega}_r^{ca} + \boldsymbol{\omega}_r^{ai} \quad (34)$$

This is analogous to the calculation of each rotation matrix to get from \mathcal{F}_i to \mathcal{F}_r in the previous section.

We begin by defining the orbital rate vector in \mathcal{F}_o . Since we are assuming that the orbit is circular, the orbital rate vector is just the mean motion of the orbit expressed as

$$\boldsymbol{\omega}_o^{oi} = \left[0 \quad -\sqrt{\mu/\|\mathbf{r}_{si}^3\|} \quad 0 \right]^T \quad (35)$$

The superscript oi denotes the angular velocity of \mathcal{F}_o with respect to \mathcal{F}_i , the subscript o shows that the rate vector is expressed in \mathcal{F}_o , and μ is the earth's gravitational parameter.

Since \mathcal{F}_a and \mathcal{F}_o change with time, we need to calculate the angular velocity $\boldsymbol{\omega}_a^{ao}$. It is not difficult to show¹¹ that $\boldsymbol{\omega}_a^{ao}$ can be calculated based on the differentiation of \mathbf{R}^{ao} as

$$\boldsymbol{\omega}_a^{ao \times} = -\overset{\circ}{\mathbf{R}}^{ao} \mathbf{R}^{oa} \quad (36)$$

where “ \circ ” denotes differentiation with respect to a moving coordinate frame. The matrix $\overset{\circ}{\mathbf{R}}^{ao}$ is found by first rewriting Eqs. (22)–(24) as

$$D_1 \hat{\mathbf{a}}_{1o} = \mathbf{r}_{t/so} \quad (37)$$

$$D_2 \hat{\mathbf{a}}_{3o} = \mathbf{r}_{t/so}^\times \mathbf{s}_o \quad (38)$$

$$\hat{\mathbf{a}}_{2o} = \hat{\mathbf{a}}_{3o}^\times \hat{\mathbf{a}}_{1o} \quad (39)$$

where the scalar quantities D_1 and D_2 are given by $\|\mathbf{r}_{t/so}\|$ and $\|\mathbf{r}_{t/so}^\times \hat{\mathbf{s}}_o\|$, respectively. Differentiating the above equations with respect to time results in the following

$$\dot{\hat{\mathbf{a}}}_{1o} = \frac{\dot{\mathbf{r}}_{t/so} - \dot{D}_1 \hat{\mathbf{a}}_{1o}}{D_1} \quad (40)$$

$$\dot{\hat{\mathbf{a}}}_{3o} = \frac{\dot{\mathbf{r}}_{t/so}^\times \hat{\mathbf{s}}_o - \dot{D}_2 \hat{\mathbf{a}}_{3o}}{D_2} \quad (41)$$

$$\dot{\hat{\mathbf{a}}}_{2o} = \hat{\mathbf{a}}_{3o}^\times \dot{\hat{\mathbf{a}}}_{1o} + \dot{\hat{\mathbf{a}}}_{3o}^\times \hat{\mathbf{a}}_{1o} \quad (42)$$

where the above has been simplified by noticing that the sun vector slowly varies in the inertial frame, and can be assumed to be fixed throughout the spacecraft trajectory thus, eliminating $\dot{\hat{\mathbf{s}}}_o$. The rates of change of D_1 and D_2 are

$$\dot{D}_1 = \frac{\dot{\mathbf{r}}_{t/so} \cdot \mathbf{r}_{t/so}}{D_1} \quad (43)$$

$$\dot{D}_2 = \frac{(\dot{\mathbf{r}}_{t/so}^\times \hat{\mathbf{s}}_o) \cdot (\mathbf{r}_{t/so}^\times \hat{\mathbf{s}}_o)}{D_2} \quad (44)$$

These time derivatives have been computed with respect to \mathcal{F}_i . We need the time derivatives with respect to the moving orbital frame, which we find by making use of the following velocity equation from analytical dynamics¹⁶

$$\dot{\mathbf{v}} = \overset{\circ}{\mathbf{v}} + \boldsymbol{\omega}^\times \mathbf{v} \quad (45)$$

where \mathbf{v} represents any vector expressed in a frame with angular velocity $\boldsymbol{\omega}$. We write the expressions for the unit vector rates of change with respect to \mathcal{F}_o as

$$\overset{\circ}{\hat{\mathbf{a}}}_{1o} = \dot{\hat{\mathbf{a}}}_{1o} - \boldsymbol{\omega}_o^{oi \times} \mathbf{a}_{1o} \quad (46)$$

$$\overset{\circ}{\hat{\mathbf{a}}}_{3o} = \dot{\hat{\mathbf{a}}}_{3o} - \boldsymbol{\omega}_o^{oi \times} \mathbf{a}_{3o} \quad (47)$$

$$\overset{\circ}{\hat{\mathbf{a}}}_{2o} = \overset{\circ}{\hat{\mathbf{a}}}_{3o}^\times \hat{\mathbf{a}}_{1o} + \hat{\mathbf{a}}_{3o}^\times \overset{\circ}{\hat{\mathbf{a}}}_{1o} \quad (48)$$

and then the rate of change of \mathbf{R}^{ao} with respect to \mathcal{F}_o is simply

$$\overset{\circ}{\mathbf{R}}^{ao} = \begin{bmatrix} \overset{\circ}{\hat{\mathbf{a}}}_{1o} & \overset{\circ}{\hat{\mathbf{a}}}_{2o} & \overset{\circ}{\hat{\mathbf{a}}}_{3o} \end{bmatrix}^T \quad (49)$$

Using Eq. (36), the angular velocity $\boldsymbol{\omega}_a^{ai}$ is then found to be

$$\boldsymbol{\omega}_a^{ai} = \boldsymbol{\omega}_a^{ao} + \mathbf{R}^{ao} \boldsymbol{\omega}_o^{oi} \quad (50)$$

It can be seen from Eq. (31) that $\boldsymbol{\omega}_a^{ca}$ is simply

$$\boldsymbol{\omega}_a^{ca} = \begin{bmatrix} \dot{\theta}_{ac} & 0 & 0 \end{bmatrix}^T \quad (51)$$

and $\dot{\theta}_{ac}$ is found by taking a time derivative of Eq.(32) to yield

$$\dot{\theta}_{ac} = \frac{-\dot{s}_{1a} p_{1c} - \dot{s}_{2a} p_{2c} \cos \theta_{ac}}{s_{2a} p_{2c} \sin \theta_{ac}} \quad (52)$$

where the derivative of the sun vector with respect to \mathcal{F}_a is given by

$$\overset{\circ}{\hat{\mathbf{s}}}_a = -\boldsymbol{\omega}_a^{ai \times} \hat{\mathbf{s}}_a \quad (53)$$

The frame \mathcal{F}_c has a fixed orientation with respect to \mathcal{F}_r , so $\boldsymbol{\omega}_r^{rc} = \mathbf{0}$. As a result, the desired tracking body rate vector $\boldsymbol{\omega}_r^{ri}$ is constructed by adding Eqs. (50) and (51), and then rotating them into the reference frame to get

$$\boldsymbol{\omega}_r^{ri} = \mathbf{R}^{ra} (\boldsymbol{\omega}_a^{ca} + \boldsymbol{\omega}_a^{ai}) \quad (54)$$

where \mathbf{R}^{ra} is the rotation matrix from \mathcal{F}_a to \mathcal{F}_r and is found from the previous section to be

$$\mathbf{R}^{ra} = \mathbf{R}^{rc} [\mathbf{R}^{ac}]^T \quad (55)$$

Once the angular rates are known in each of the coordinate frames, we compute the desired angular accelerations. The accelerations are needed to compute the reference axial wheel torque \mathbf{g}_{ar} to generate the desired trajectory. The

angular acceleration $\dot{\omega}_r^{ri}$ is constructed analogously to the angular velocity ω_r^{ri} by differentiating Eqs. (33–53). The acceleration commands are found by taking a time derivative of Eq. (33)

$$\ddot{\mathbf{r}}_{t/si} = \ddot{\mathbf{r}}_{ti} - \ddot{\mathbf{r}}_{si} \quad (56)$$

Here $\ddot{\mathbf{r}}_{si}$ is simply the two-body equation of motion¹⁷ given as

$$\ddot{\mathbf{r}}_{si} = -\frac{\mu}{\|\mathbf{r}_{si}\|^3} \mathbf{r}_{si} \quad (57)$$

It can be shown from basic kinematics¹⁸ and from Ref. 5 that the inertial acceleration of the target $\ddot{\mathbf{r}}_{ti}$ is

$$\ddot{\mathbf{r}}_{ti} = \frac{\omega_E^2 \mathbf{r}_{ti}}{\|\mathbf{r}_{ti}\|} \hat{\mathbf{n}}_t + \|\mathbf{r}_{ti}\| \omega_e^2 \hat{\mathbf{u}}_t \quad (58)$$

where $\hat{\mathbf{n}}_t$ and $\hat{\mathbf{u}}_t$ are the normal and tangential unit vectors of the target motion.

The angular acceleration $\dot{\omega}_o^{oi}$ is found by differentiating Eq. (35):

$$\dot{\omega}_o^{oi} = \left[0 \quad 1.5\mu / \left(\|\mathbf{r}_{si}^4\| \sqrt{\mu / \|\mathbf{r}_{si}^3\|} \right) \quad 0 \right]^T \quad (59)$$

The angular acceleration $\dot{\omega}_a^{ao}$ is found by differentiating Eq. (36) which yields

$$\dot{\omega}_a^{ao \times} = -\ddot{\mathbf{R}}^{ao} \mathbf{R}^{oa} - \dot{\mathbf{R}}^{ao} \dot{\mathbf{R}}^{oa} \quad (60)$$

The second derivative of \mathbf{R}^{ao} is found by differentiating Eqs. (46–48):

$$\overset{\circ\circ}{\hat{\mathbf{a}}}_{1o} = \overset{\circ\circ}{\hat{\mathbf{a}}}_{1o} - 2\omega_o^{oi \times} \overset{\circ}{\hat{\mathbf{a}}}_{1o} - \omega_o^{oi \times} (\omega_o^{oi \times} \overset{\circ}{\hat{\mathbf{a}}}_{1o}) - \dot{\omega}_o^{oi \times} \overset{\circ}{\hat{\mathbf{a}}}_{1o} \quad (61)$$

$$\overset{\circ\circ}{\hat{\mathbf{a}}}_{3o} = \overset{\circ\circ}{\hat{\mathbf{a}}}_{3o} - 2\omega_o^{oi \times} \overset{\circ}{\hat{\mathbf{a}}}_{3o} - \omega_o^{oi \times} (\omega_o^{oi \times} \overset{\circ}{\hat{\mathbf{a}}}_{3o}) - \dot{\omega}_o^{oi \times} \overset{\circ}{\hat{\mathbf{a}}}_{3o} \quad (62)$$

$$\overset{\circ\circ}{\hat{\mathbf{a}}}_{2o} = \overset{\circ\circ \times}{\hat{\mathbf{a}}}_{3o} \overset{\circ}{\hat{\mathbf{a}}}_{1o} + 2 \overset{\circ \times}{\hat{\mathbf{a}}}_{3o} \overset{\circ}{\hat{\mathbf{a}}}_{1o} + \overset{\circ \times}{\hat{\mathbf{a}}}_{3o} \overset{\circ\circ}{\hat{\mathbf{a}}}_{1o} \quad (63)$$

$$\overset{\circ\circ}{\mathbf{R}}^{ao} = \left[\overset{\circ\circ}{\hat{\mathbf{a}}}_{1o} \quad \overset{\circ\circ}{\hat{\mathbf{a}}}_{2o} \quad \overset{\circ\circ}{\hat{\mathbf{a}}}_{3o} \right]^T \quad (64)$$

where the inertial derivatives of the unit vectors are found by differentiating Eqs. (40–41):

$$\overset{\circ\circ}{\hat{\mathbf{a}}}_{1o} = \frac{\ddot{\mathbf{r}}_{t/so} - 2\dot{D}_1 \overset{\circ}{\hat{\mathbf{a}}}_{1o} - \ddot{D}_1 \overset{\circ}{\hat{\mathbf{a}}}_{1o}}{D_1} \quad (65)$$

$$\overset{\circ\circ}{\hat{\mathbf{a}}}_{3o} = \frac{\ddot{\mathbf{r}}_{t/so}^\times \mathbf{S}_o - 2\dot{D}_2 \overset{\circ}{\hat{\mathbf{a}}}_{3o} - \ddot{D}_2 \overset{\circ}{\hat{\mathbf{a}}}_{3o}}{D_2} \quad (66)$$

$$\ddot{D}_1 = \frac{(\ddot{\mathbf{r}}_{t/so} \cdot \mathbf{r}_{t/so}) + (\dot{\mathbf{r}}_{t/so} \cdot \dot{\mathbf{r}}_{t/so}) - \dot{D}_1^2}{D_1} \quad (67)$$

$$\ddot{D}_2 = \frac{(\ddot{\mathbf{r}}_{t/so}^\times \hat{\mathbf{S}}_o) \cdot (\mathbf{r}_{t/so}^\times \hat{\mathbf{S}}_o) + (\dot{\mathbf{r}}_{t/so}^\times \hat{\mathbf{S}}_o) \cdot (\mathbf{r}_{t/so}^\times \hat{\mathbf{S}}_o) - \dot{D}_2^2}{D_2} \quad (68)$$

and then $\dot{\omega}_a^{ai}$ becomes

$$\dot{\omega}_a^{ai} = \dot{\omega}_a^{ao} + \mathbf{R}^{ao} \dot{\omega}_o^{oi} \quad (69)$$

Likewise, $\dot{\omega}_a^{ca}$ is found by differentiating the expression in Eq. (51) where

$$\ddot{\theta}_{ac} = \frac{-\ddot{s}_{1a} p_{1c} + 2\ddot{\theta}_{ac} \dot{s}_{2a} p_{2c} \sin \theta_{ac} - \ddot{s}_{2a} p_{2c} \cos \theta_{ac}}{s_{2a} p_{2c} \sin \theta_{ac}} \quad (70)$$

and the acceleration of the sun vector with respect to \mathcal{F}_a is given by

$$\overset{\circ}{\hat{\mathbf{s}}}_a = -2\boldsymbol{\omega}_a^{ai \times} \overset{\circ}{\hat{\mathbf{s}}}_a - \boldsymbol{\omega}_a^{ai \times} (\boldsymbol{\omega}_a^{ai \times} \hat{\mathbf{s}}_a) \quad (71)$$

The desired angular acceleration becomes

$$\dot{\boldsymbol{\omega}}_r^{ri} = \mathbf{R}^{ra} (\overset{\circ}{\boldsymbol{\omega}}_a^{ca} + \dot{\boldsymbol{\omega}}_a^{ai}) \quad (72)$$

where as before, \mathbf{R}^{ra} is the rotation matrix from \mathcal{F}_a to \mathcal{F}_r . Like the desired angular velocity vector $\boldsymbol{\omega}_r^{ri}$, the desired acceleration vector $\dot{\boldsymbol{\omega}}_r^{ri}$ is constructed from knowing $\overset{\circ}{\boldsymbol{\omega}}_a^{ca}$ and $\dot{\boldsymbol{\omega}}_a^{ai}$ in \mathcal{F}_r using Eq. (55). Having now found \mathbf{R}^{ri} , $\boldsymbol{\omega}_r^{ri}$, and $\dot{\boldsymbol{\omega}}_r^{ri}$, we can completely describe the desired trajectory that the real spacecraft needs to have in order to track a target. In the next section, we show how this open-loop reference trajectory is used to derive a control law that will asymptotically drive any initial attitude and rate errors in the body frame to zero.

CONTROLLERS

The nonlinear feedback controller presented in this paper uses momentum wheels to generate the internal axial torque \mathbf{g}_a . Here, the wheels are the only devices used to track rigid spacecraft attitude motions and to correct tracking errors. Thrusters were used in Ref. 7 to track the attitude motions while momentum wheels corrected for tracking errors. The only external torque is the gravity gradient torque \mathbf{g}_e . Like the controllers used in Ref. 7, this feedback controller globally asymptotically stabilizes the tracking error through the use of a Lyapunov function.

Error Kinematics

We define the tracking error kinematics between the body and reference frames. The attitude tracking error is defined by

$$\mathbf{R}^{br}(\boldsymbol{\delta}\boldsymbol{\sigma}) = \mathbf{R}^{bi}(\boldsymbol{\sigma}_b)\mathbf{R}^{ir}(\boldsymbol{\sigma}_r) \quad (73)$$

with $\mathbf{R}^{br}(\boldsymbol{\delta}\boldsymbol{\sigma})$ being the rotation matrix from the reference frame \mathcal{F}_r to the body frame \mathcal{F}_b , and $\boldsymbol{\delta}\boldsymbol{\sigma}$ is the error in the attitude between the frames \mathcal{F}_b and \mathcal{F}_r . The tracking error of the angular velocity expressed in \mathcal{F}_b as

$$\boldsymbol{\delta}\boldsymbol{\omega} = \boldsymbol{\omega}_b - \mathbf{R}^{br}(\boldsymbol{\delta}\boldsymbol{\sigma})\boldsymbol{\omega}_r \quad (74)$$

Using Eq. (3), the differential equation for the error kinematics becomes

$$\boldsymbol{\delta}\dot{\boldsymbol{\sigma}} = \mathbf{G}(\boldsymbol{\delta}\boldsymbol{\sigma})\boldsymbol{\delta}\boldsymbol{\omega} \quad (75)$$

With these three relations, we are now ready to derive the control law in the next section.

The Feedback Tracking Controller

The feedback momentum wheel controller is derived from Lyapunov control theory. We use the following Lyapunov function candidate⁷

$$V = \frac{1}{2}\boldsymbol{\delta}\boldsymbol{\omega}^T \mathbf{K}\boldsymbol{\delta}\boldsymbol{\omega} + 2k_2 \ln(1 + \boldsymbol{\delta}\boldsymbol{\sigma}^T \boldsymbol{\delta}\boldsymbol{\sigma}) \quad (76)$$

where k_2 is some positive gain constant. Substituting Eq. (74) into Eq. (76) and taking the derivative, yields the following equation for \dot{V} in terms of $\boldsymbol{\omega}_b$, $\boldsymbol{\omega}_r$, and the tracking errors $\boldsymbol{\delta}\boldsymbol{\sigma}$ and $\boldsymbol{\delta}\boldsymbol{\omega}$:

$$\dot{V} = \left[\dot{\boldsymbol{\omega}}_b - \dot{\mathbf{R}}^{br}(\boldsymbol{\delta}\boldsymbol{\sigma})\boldsymbol{\omega}_r - \mathbf{R}^{br}(\boldsymbol{\delta}\boldsymbol{\sigma})\dot{\boldsymbol{\omega}}_r \right]^T \mathbf{K}\boldsymbol{\delta}\boldsymbol{\omega} + k_2 \frac{\boldsymbol{\delta}\boldsymbol{\sigma}^T \boldsymbol{\delta}\dot{\boldsymbol{\sigma}}}{1 + \boldsymbol{\delta}\boldsymbol{\sigma}^T \boldsymbol{\delta}\boldsymbol{\sigma}} \quad (77)$$

We rewrite Eq. (77), using Eqs. (1) and (75), as

$$\dot{V} = \left[\mathbf{J}^{-1} (\mathbf{h}_b^\times \boldsymbol{\omega}_b + \mathbf{g}_e - \mathbf{A}\mathbf{g}_a) - \boldsymbol{\omega}_b^\times \boldsymbol{\delta}\boldsymbol{\omega} - \mathbf{R}^{br}(\boldsymbol{\delta}\boldsymbol{\sigma})\mathbf{J}^{-1} (\mathbf{h}_r^\times \boldsymbol{\omega}_r + \mathbf{g}_e - \mathbf{A}\mathbf{g}_{ar}) \right]^T \mathbf{K}\boldsymbol{\delta}\boldsymbol{\omega} + k_2 \boldsymbol{\delta}\boldsymbol{\sigma}^T \boldsymbol{\delta}\boldsymbol{\omega} \quad (78)$$

where we have made use of the fact proved in Ref. 7

$$\frac{d\mathbf{R}^{br}(\boldsymbol{\delta}\boldsymbol{\sigma})}{dt} \boldsymbol{\omega}_r = \boldsymbol{\omega}_b^\times \boldsymbol{\delta}\boldsymbol{\omega} \quad (79)$$

Letting $\mathbf{K} = \mathbf{J}$ in Eq. (78) and making use of Eq. (7), the final equation for the derivative of V becomes:

$$\begin{aligned}\dot{V} = & -[-\mathbf{h}_b^\times \mathbf{J}^{-1}(\mathbf{h}_b - \mathbf{A}\mathbf{h}_a) - \mathbf{g}_e + \mathbf{A}\mathbf{g}_a + \mathbf{J}\boldsymbol{\omega}_b^\times \delta\boldsymbol{\omega} \\ & + \mathbf{J}\mathbf{R}^{br}(\delta\boldsymbol{\sigma})\mathbf{J}^{-1}\mathbf{h}_r^\times \mathbf{J}^{-1}(\mathbf{h}_r - \mathbf{A}\mathbf{h}_{ar}) + \mathbf{J}\mathbf{R}^{br}(\delta\boldsymbol{\sigma})\mathbf{J}^{-1}\mathbf{g}_e \\ & - \mathbf{J}\mathbf{R}^{br}(\delta\boldsymbol{\sigma})\mathbf{J}^{-1}\mathbf{A}\mathbf{g}_{ar} - k_2\delta\boldsymbol{\sigma}]^T \delta\boldsymbol{\omega}\end{aligned}\quad (80)$$

We want to choose the control torques $\mathbf{A}\mathbf{g}_a$ so that \dot{V} is negative definite. Choosing

$$\begin{aligned}\mathbf{A}\mathbf{g}_a = & \mathbf{h}_b^\times \mathbf{J}^{-1}(\mathbf{h}_b - \mathbf{A}\mathbf{h}_a) + \mathbf{g}_e - \mathbf{J}\boldsymbol{\omega}_b^\times \delta\boldsymbol{\omega} \\ & - \mathbf{J}\mathbf{R}^{br}(\delta\boldsymbol{\sigma})\mathbf{J}^{-1}\mathbf{h}_r^\times \mathbf{J}^{-1}(\mathbf{h}_r - \mathbf{A}\mathbf{h}_{ar}) - \mathbf{J}\mathbf{R}^{br}(\delta\boldsymbol{\sigma})\mathbf{J}^{-1}\mathbf{g}_e \\ & + \mathbf{J}\mathbf{R}^{br}(\delta\boldsymbol{\sigma})\mathbf{J}^{-1}\mathbf{A}\mathbf{g}_{ar} + k_1\delta\boldsymbol{\omega} + k_2\delta\boldsymbol{\sigma}\end{aligned}\quad (81)$$

where k_1 is a positive gain constant leads to

$$\dot{V} = -k_1\delta\boldsymbol{\omega}^T \delta\boldsymbol{\omega} \leq 0 \quad (82)$$

As found in Ref. 7, it can be shown that the control law in Eq. (81) guarantees perfect tracking, i.e., $\boldsymbol{\omega}_b(t) = \boldsymbol{\omega}_r(t)$ and $\boldsymbol{\sigma}_b(t) = \boldsymbol{\sigma}_r(t)$ for all $t \geq 0$ if the initial condition errors are zero, i.e., $\delta\boldsymbol{\omega}(0) = \delta\boldsymbol{\sigma}(0) = 0$.

NUMERICAL EXAMPLE

We demonstrate the capability of the momentum wheel control law by presenting a target tracking example. Given a circular orbit with an altitude of 279.24 km, we want to a spacecraft to acquire and track Cape Canaveral, Florida ($\delta_t = 28.467^\circ N$, $L_t = 80.467^\circ W$) starting with a sub-satellite point located at $19.583^\circ N$ longitude and $118.381^\circ W$ longitude. Here, our algorithms do not determine whether or not the target is actually visible by the sensor. We will assume, for this example, that the spacecraft can see the target. The spacecraft is modeled as a gyrostat with three momentum wheels aligned with the principal axes. Their axial moments of inertia are given as

$$\mathbf{I}_s = \text{diag}(10, 30, 70) \quad (83)$$

We let the spacecraft total moment of inertia matrix (platform and momentum wheels) be

$$\mathbf{J} = \text{diag}(200, 150, 175) \quad (84)$$

and the solar panel unit vector $\hat{\mathbf{p}}$ is defined in \mathcal{F}_b as

$$\hat{\mathbf{p}} = [0.5437 \ 0.8269 \ 0.1440]^T \quad (85)$$

The spacecraft actual initial attitude is $\boldsymbol{\sigma}_b(0) = [-0.1259 \ 0.2598 \ -0.0988]^T$ with its sensor boresight initially pointing at $24.737^\circ N$ longitude and $100.435^\circ W$ longitude. We let the platform initially rotate with $\boldsymbol{\omega}_b(0) = [-0.0040 \ -0.00854 \ 0.0009]^T$.

The target tracking maneuver results are shown in Figs. 3, 4, and 5. The gains⁷ for the controller were chosen to be $k_1 = 54$ and $k_2 = 47$.

Figure 3(a) shows the time history of $\delta\boldsymbol{\sigma}$, and Figure 3(b) shows the time history of $\delta\boldsymbol{\omega}$. It can be seen that the controller does indeed make the body frame track the prescribed reference trajectory. All of the attitude and rate errors were driven asymptotically to zero over time. Figure 4(a) shows the control torque generated by the controller. The controller initially generates large torques to slew the spacecraft to point at the target. Once the target has been acquired, which means all errors are zero, the torques needed to track the target become very small and equal to \mathbf{g}_{ar} . Figure 4(b) illustrates the ideal torque \mathbf{g}_{ar} needed for target tracking if all there are no initial errors. Figure 5 illustrates the yaw-steering condition of Eq. (16). It is clearly seen that the solar panel axis becomes normal to the sun

vector about the same time the spacecraft acquires the target (40 sec.). Thus, Figure 5 indicates that the spacecraft can simultaneously a target while maintaining its power requirements.

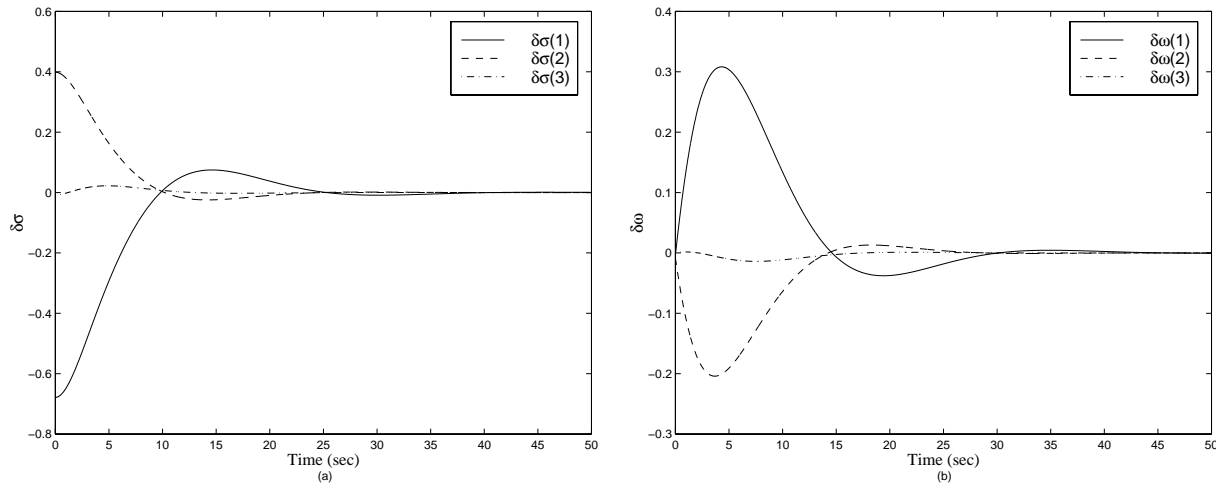


Figure 3: The time history of (a) $\delta\sigma$ and (b) $\delta\omega$.

CONCLUSIONS

A method for computing a multi-axis target tracking trajectory has been developed that also allows the solar panel normal to be aligned with the sun vector during a tracking maneuver. Other authors have developed similar algorithms, but the open-loop trajectory in this paper is attitude parameter independent with the sun tracking requirement incorporated. A control law has been developed that uses internal torques provided by the momentum wheels for tracking rotational maneuvers. The control law is a function of the spacecraft angular momentum, wheel momenta, and attitude, as well as the desired pointing direction. A simple tracking maneuver example clearly shows that the wheel controller makes the body frame track the reference motion.

REFERENCES

- [1] Gramling, C. J., Lee, T., Niklewski, D. J., and Long, A. C., "Relative Navigation For Autonomous Formation Flying Of Spacecraft," In *Proceedings of the AAS/AIAA 1997 Astrodynamics Specialist Conference*, 1997.
- [2] DeCou, A. B., "Orbital Station-Keeping for Multiple Spacecraft Interferometry," *Journal of the Astronautical Sciences*, Vol. 39, No. 3, 1991, pp. 283–297.
- [3] Ulybyshev, Y., "Long-Term Formation Keeping of Satellite Constellation Using Linear-Quadratic Controller," *Journal of Guidance, Control, and Dynamics*, Vol. 21, No. 1, 1998, pp. 109–115.
- [4] Folta, D., Bordi, F., and Scolese, C., "Considerations On Formation Flying Separations For Earth Observing Satellite Missions," *Advances in Astronautical Sciences*, Vol. 79, No. 2, 1992, pp. 803–822.
- [5] Hablani, H. B., "Design of a Payload Pointing Control System for Tracking Moving Objects," *Journal of Guidance, Control, and Dynamics*, Vol. 12, No. 3, 1989, pp. 365–374.
- [6] Hablani, H. B., "Multi-axis Tracking and Attitude Control of Flexible Spacecraft with Reaction Jets," *Journal of Guidance, Control, and Dynamics*, Vol. 17, No. 4, 1994, pp. 831–839.
- [7] Hall, C. D., Tsiotras, P., and Shen, H., "Tracking Rigid Body Motion Using Thrusters and Momentum Wheels," In *1998 AIAA/AAS Astrodynamics Conference*, August 1998.

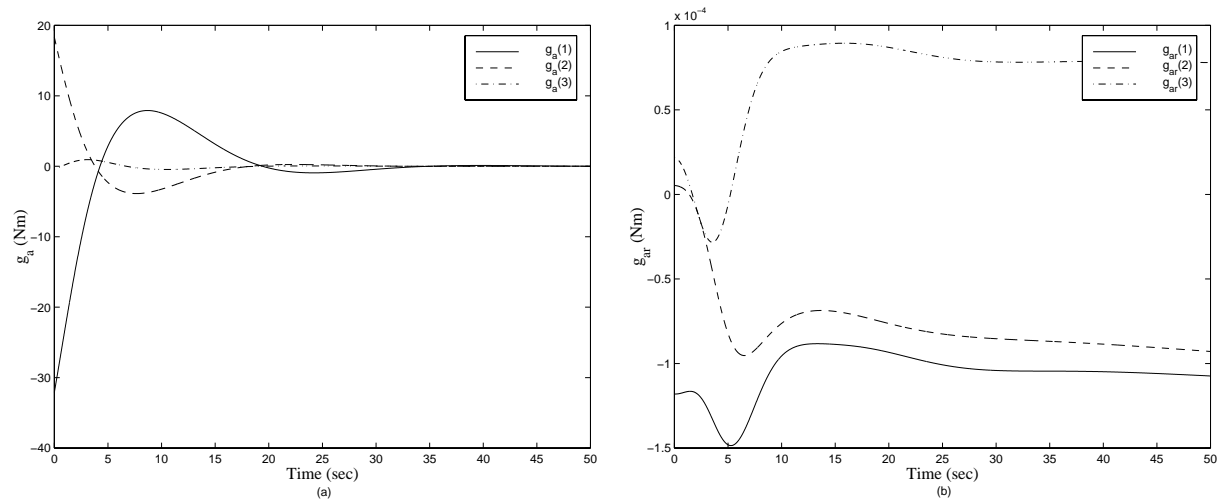


Figure 4: (a) The momentum wheel feedback control law in Eq. 81, and (b) The desired control for target tracking.

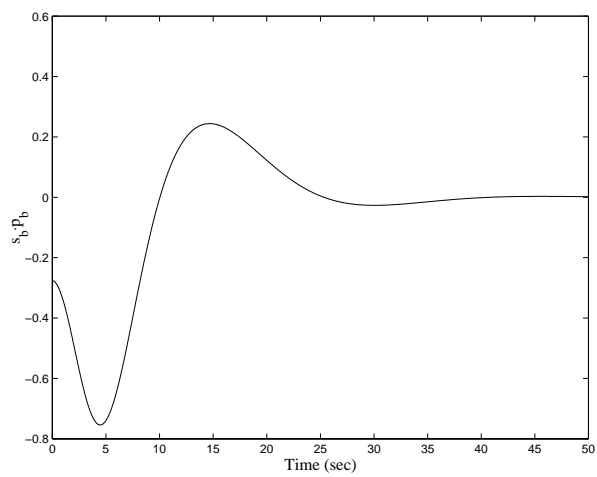


Figure 5: The yaw-steering condition of Eq. (16).

- [8] Schaub, H., Robinett, R. D., and Junkins, J. L., "Globally Stable Feedback Laws for Near-Minimum-Fuel and Near-Minimum-Time Pointing Maneuvers for a Landmark-Tracking Spacecraft," *Journal of the Astronautical Sciences*, Vol. 44, No. 4, 1996, pp. 443–466.
- [9] Steyn, W. H., "Near-Minimum-Time Eigenaxis Rotation Maneuvers Using Reaction Wheels," *Journal of Guidance, Control and Dynamics*, Vol. 18, No. 5, 1995, pp. 1184–1189.
- [10] Wie, B. and Lu, J., "Feedback Control Logic for Spacecraft Eigenaxis Rotations Under Slew Rate and Control Constraints," *Journal of Guidance, Control and Dynamics*, Vol. 18, No. 6, 1995, pp. 1372–1379.
- [11] Hughes, P. C., *Spacecraft Attitude Dynamics*, John Wiley & Sons, New York, 1986.
- [12] Hall, C. D., "Spinup Dynamics of Gyrostats," *Journal of Guidance, Control, and Dynamics*, Vol. 18, No. 5, 1995, pp. 1177–1183.
- [13] Wertz, J., editor, *Spacecraft Attitude Determination and Control*, D. Reidel, Dordrecht, Holland, 1978.
- [14] Shuster, M. D., "A Survey of Attitude Representations," *Journal of the Astronautical Sciences*, Vol. 41, No. 4, 1993, pp. 439–517.
- [15] Kalweit, C. C., "Optimum Yaw Motion for Satellites with a Nadir-Pointing Payload," *Journal of Guidance, Control, and Dynamics*, Vol. 6, No. 1, 1983, pp. 47–52.
- [16] Meirovitch, L., *Methods of Analytical Dynamics*, McGraw-Hill, New York, 1970.
- [17] Vallado, D. A., *Fundamentals of Astrodynamics and Applications*, McGraw-Hill, New York, 1997.
- [18] Meriam, J. L. and Kraige, L., *Dynamics (SI Version)*, John Wiley & Sons, New York, third edition, 1992.